

A Novel Method Based on Learning Automata for Automatic Lesion Detection in Breast Magnetic Resonance Imaging

Leila Salehi, Reza Azmi

Department of Computer Engineering, Alzahra University, Tehran, Iran

Submission: 09-06-2013 Accepted: 16-04-2014

ABSTRACT

Breast cancer continues to be a significant public health problem in the world. Early detection is the key for improving breast cancer prognosis. In this way, magnetic resonance imaging (MRI) is emerging as a powerful tool for the detection of breast cancer. Breast MRI presently has two major challenges. First, its specificity is relatively poor, and it detects many false positives (FPs). Second, the method involves acquiring several high-resolution image volumes before, during, and after the injection of a contrast agent. The large volume of data makes the task of interpretation by the radiologist both complex and time-consuming. These challenges have led to the development of the computer-aided detection systems to improve the efficiency and accuracy of the interpretation process. Detection of suspicious regions of interests (ROIs) is a critical preprocessing step in dynamic contrast-enhanced (DCE)-MRI data evaluation. In this regard, this paper introduces a new automatic method to detect the suspicious ROIs for breast DCE-MRI based on region growing. The results indicate that the proposed method is thoroughly able to identify suspicious regions (accuracy of 75.39 ± 3.37 on PIDER breast MRI dataset). Furthermore, the FP per image in this method is averagely 7.92, which shows considerable improvement comparing to other methods like ROI hunter.

Key words: Breast cancer, learning automata, local binary pattern, magnetic resonance imaging, region of interest detection

INTRODUCTION

Breast cancer is the most common cancer among women. It is also the second cause of cancer deaths among women and it is included 15% of cancer deaths.^[1] In this regard, the key point to increase the survival rate and life expectancy is early detection of the disease and its treatment.

Medical imaging plays a vital role in the cure of breast cancer, detection, diagnosis, treatment planning, and assessment of treatment response. Currently, mammography is the primary screening method for detecting of breast cancer. Unfortunately, 10-30% of breast cancers aren't detected by mammography^[2-4] and positive predictive value of mammography is <35%.^[5] Therefore, other imaging techniques such as magnetic resonance imaging (MRI),^[6,7] ultrasound,^[8,9] and nuclear medicine imaging^[10,11] are used as an adjunct screening method for patients with or suspected to breast cancer. Some studies show the superiority of MRI compared to mammography and ultrasound images in order to determine tumor volume.^[12,13]

Today, interpretation of breast MRI is one of the most challenging issues in the field of medical image processing.

Manual interpretation of breast cancer is a boring and time-consuming work. There is a great interest to use computer-aided detection (CAD) and diagnosis systems that are capable of increasing the efficiency, accuracy, and consistency of breast MRI interpretation. In computer-aided systems, detection of the suspected region of interest (ROI) is the essential stage for determining the exact volume of tumor. The significant point in this way is that the selection of suspicious ROI is completely depended on the operator. In addition, because of high volume and multi-dimensional data of dynamic contrast-enhanced (DCE)-MRI datasets, it inadvertently causes the elimination of the regions containing tumor.^[14,15] Therefore, using fully automatic interpretation of MRI and choosing the reliable and right ROI eliminates human interactions and also can be more useful and valuable than the manual or semi-automatic methods.

Based on the above-mentioned, several studies have conducted various methods to directly segmented breast lesions. In^[16] a two-stage thresholding method is used. A threshold detects enhancement region from the background and the second threshold detects the suspected region from enhanced area. Hayton^[17] used a segmentation

Address for correspondence:

Leila Salehi, Department of Computer Engineering, Alzahra University, Tehran, Iran. E-mail: salehi.leili@gmail.com

method based on thresholding of an image that obtained by subtracting two pre- and post-contrast images. This survey uses three different thresholds: A constant threshold, threshold derived from a histogram, and threshold defined as some percentage of the maximum value in the data. Since the signal intensity of MRI is depended on the contrast agent and also it needs particular MRI instrument, there is no general method for selecting the threshold and therefore the performance of these methods require user interaction.

Gihuijs *et al.*^[18] proposed a region growing seed-based algorithm to segment the lesion from the ROIs. These ROIs are achieved from threshold that is derived from the histogram of an image. In this method, the seeds manually are selected by the user. In addition, the same tissues may not behave uniformly against contrast agent and so this reduces accuracy of the threshold-based methods. Lucht *et al.*^[19] used pharmacokinetic modeling to produce parametric maps that were used for manual ROI selection; however, the computation of tracer kinetic parameters is still a lengthy task when performed on entire images. Gal *et al.*^[15] proposed a region growing method based on intensity value in the original image and fitted pharmacokinetic parameters. This approach automatically selects the seed voxel using kinetic parameters (e.g. through threshold) for selecting ROI is incorrect approach because tumor heterogeneity, which is an important factor to be accounted for, could be missed.

Yan *et al.* proposed a marker-controlled watershed method to segment lymphoma in sequential computerized tomography images.^[20] In their method, the external marker is obtained manually by drawing a circle enclosing the lymphoma. The internal marker is determined automatically by combing techniques including canny edge detection, thresholding, and morphological operation. Cui *et al.* also proposed a semi-automatic method based on marker-controlled watershed transformation to segment breast lesion volumes on MRI.^[21] They manually selected the ROI in a single image, followed by a Gaussian mixture model applied to a histogram of pixels inside the ROI to distinguish the lesion class from other tissues. The internal and external marker are determined on the basis of the ROI and the intensity distribution of the lesion, and the lesion contour is delineated using a marker-controlled watershed transform. These methods hardly be applied to MRI CAD because of their semi-automatic nature.

Automatic lesion detection in breast DCE-MRI is still an open problem and only a few authors presented algorithms aiming to automate the task. Vignati *et al.*^[22] focused on automatic lesion detection, and Renz *et al.*^[23] presented an approach to automatically detect and classify breast lesions. The authors reported satisfactory results, but their studies have some limitations since the performance of the algorithms was not tested on dataset with normal DCE-MRI

studies, the proposed algorithms were only applied to mass-like lesions.^[22,23]

It should be noted that the size of breast MRI is too large. Therefore, concentration on the enhancement regions and consequently reduction of the surface under consideration results in the reduction of the segmentation complexity can be very useful. Based on this, application of an algorithm without losing meaningful information for detecting ROIs is valuable.

One of the medical image processing methods used in several surveys is ROI hunter.^[24] In this method, the whole image is scanned in order to find the maximum intensity (as the center of suspected lesion). Then, a set of concentric rings are drawn up around a local maximum until the ratio of pixel average intensity within each ring to maximum intensity is more than the threshold value.

The main disadvantage of this method is that the seed points are selected without considering their neighbors. Furthermore, the performance of the method is depended on threshold values.

In this paper, a novel automatic algorithm to detect ROI is proposed. This method is based on region growing, and it estimates the radius of ROI using learning automata (LA). Furthermore, in order to overcome the weakness of earlier contributions, learning methods are utilized to find the best of primary seed set.

METHODS

The framework of this method is the development of the new method acting as a support to the detection process for medical imaging and satisfies those requirements. Our first contribution dealing with the segmentation suspicious lesion was concentrated on the idea of the manual detection of suspicious ROI by radiologist.^[25] To extend previous research, this paper has proposed an automatic method for detecting suspicious ROI based on the automatic seed selection and region growing in breast MRI. At the first step, it applied the thresholding to select the seeds from the postcontrast MRI. After that the best seeds were selected considering their neighborhood by using local binary pattern (LBP) features and learning method. At the second step detecting suspicious ROI through region growing/merging by use of LA. Figure 1 shows an overall view of this approach.

Seed Selection

A seed point is the starting point for region growing. Selection of the seed point significantly affects the segmentation result. Selecting a seed point outside the ROI will lead to incorrect results.

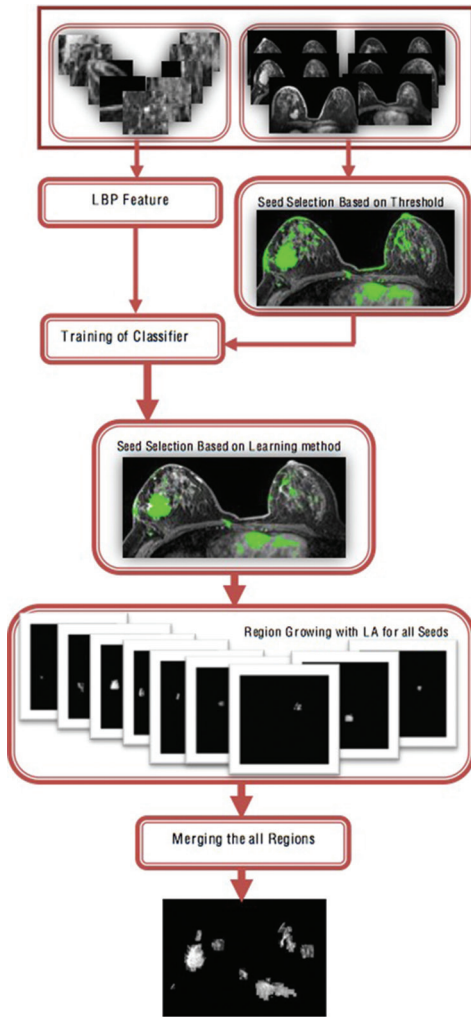


Figure 1: Illustration of the proposed approach

Step 1: Seed Selection Based on Thresholding

There are several different methods to choose a threshold. Threshold can be chosen manually, or through an algorithm that are automatically computed. A simple thresholding method for seed selection is to choose the mean or median value and then the pixels bigger than it are chosen as seeds. This paper utilized this algorithm to select the seeds in the first step. Since this algorithm selects the seeds without considering their neighborhoods, the next step selects the targeted seeds accurately by learning based method.

Step 2: Seeds Selection Based on Learning Methods and Local Binary Pattern Feature

- Local binary pattern feature detection

Local binary pattern was first described by Ojala *et al.*^[26,27] It is considered as an effective descriptor for texture classification. LBP operator's labels image pixels by Thresholding in the 3×3 neighborhood of each pixel with the center value and considering the result of this thresholding as a binary number.

Figure 2 shows that how the LBP codes are computed. After computing the LBP codes for all image pixels, the histogram of these codes is computed and used as texture descriptor. Limitation of this basic LBP was a small size of its neighborhood (3×3); therefore, it is unable to deal with typical features with large-scale structures. To overcome this limitation, later expanded for use in a different neighborhood.^[28]

This operator allows detection of local binary patterns at circular neighborhoods of any quantization of the angular

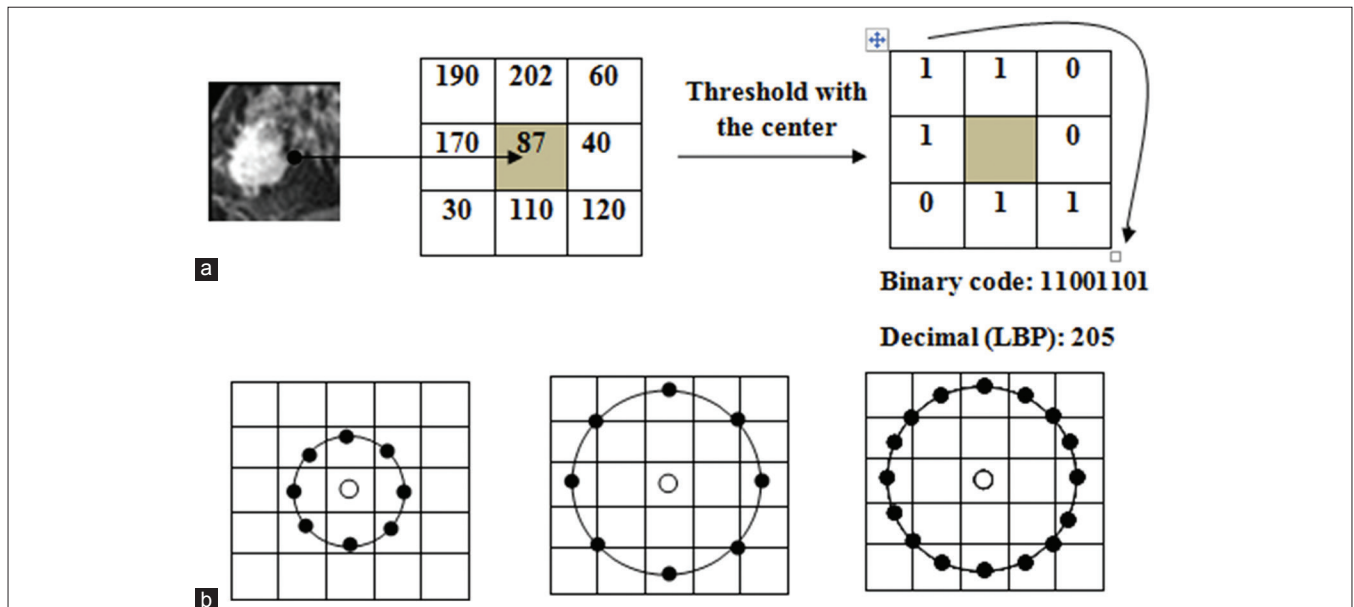


Figure 2: Local binary pattern (LBP) computation. (a) Example of the basic LBP operator. (b) Examples of the common circular LBP neighborhoods: (8,1), (8,2) and (16,2) respectively

space and at any spatial resolution. Therefore, it derives the operator for a general case-based on a circularly symmetric neighborhood of P members on a circle of radius R . In addition to evaluating the performance of individual operators of a particular configuration (P, R), one could analyze and combine the responses of multiple operators realized with different parameters (P, R).^[28]

A local binary pattern is called uniform if it contains at most two bitwise transitions from 0 to 1 or vice versa when the bit pattern is considered circular. For example, the patterns 01110000 and 100011100 are uniform and 01010010 are not.

As stated by Ojala, the uniform patterns in the (8,1) neighborhood account nearly 90% of all patterns and for about 70% in the (16,2) neighborhood in texture images. In this paper, we use the uniform LBP operator as $LBP_{P,R}^{u2}$ where the down index represents using LBP in a (P, R) neighborhood and the up index u2 shows the using of uniform patterns.

In the work of Ojala, histogram of the labeled image $f_i(x, y)$ is used as a descriptor. We can define this histogram as

$$H_i = \sum_{x,y} I(f_i(x, y) = i), \quad i = 0, \dots, n-1 \quad (1)$$

Where n is the number of different labels produced by the LBP operator, and $I(A) = 1$ when A is true, while $I(A) = 0$ when A is false.

This histogram of uniform pattern computed over an image or regions that contains information about the local micro-patterns such as edges, spots and flat areas, and has been shown to be a very powerful texture descriptor.

- Learning based seeds selection

As noted earlier, seed selection in the first step was only based on grey level. Since the MR image includes a lot of noise, false-positive (FP) of seeds collection that is derived from the first stage has a high amount.

Inherently, texture and its spatial information play a key role in correctly selecting the seeds. Due to this fact, we establish our approach on the use of LBP for considering micro-patterns in whole of seeds and adapting of these descriptors for preserving the neighborhood of the seeds. Our general procedure in this step consists of using the LBP texture descriptor to describing neighborhood of the seeds. The LBP descriptor used to reduce the FP via classifying the seeds into two categories, seeds belonging to the tumor or to the normal tissue.

In this stage, one seed randomly is selected from seeds collection. After that, a 25×25 rectangular region is considered around of seed (this seed is the center of this

region). In following of approach, LBP histogram for this region is computed and is allocated to above-mentioned central seed.

The final step of proposed approach is seed classification. To reach this goal, we use the k-nearest neighbor (k-NN) algorithm^[29] that is a nonparametric method for classifying objects based on closest training examples in the feature space. Finally, the number of seeds decreases by about 50% of primary value.

Region of Interest Detection

Detection of suspicious ROIs is a critical preprocessing step in DCE-MRI data evaluation.

Learning Automata

Learning is defined as the ability of a system to improve its responses based on past experiences.^[30] Automata is a machine that can perform a finite number of actions. Each selected action is assessed by a probabilistic environment. Response of evaluation is given in the form of a positive or negative signal to automata and then automata depending on its past experiences selected the next action. The ultimate goal of this is the automata learned to choose the best action within its actions. Each action that maximize the probability of reward token from the environment, is the best and the next action is chosen according to specific probability distribution. This probability distribution based on environment responses to automata is updated. Figure 3 represents a feedback connection of an automaton and an environment. The LA can be represented by a quintuple $\{\Phi, \alpha, \beta, F, h\}$ where:

- Φ is a set of state of automata. At any instant n , the state $\Phi(n)$ is belonging to a finite set $\Phi = \{\Phi_1, \Phi_2, \dots, \Phi_s\}$
- α is a set of action (output of automata), action of automata at instant n is $\alpha(n)$, and set of actions is $\alpha = \{\alpha_1, \alpha_2, \dots, \alpha_r\}$
- β is a set of environment responses (inputs of automata), the input of automata in instant n is $\beta(n)$ and set of inputs defined as follows: $\beta = \{\beta_1, \beta_2, \dots, \beta_m\}$, $\beta(n)$ is an element of this set
- $F: \Phi \times \beta \rightarrow \Phi$ is the learning algorithm. F is a mapping

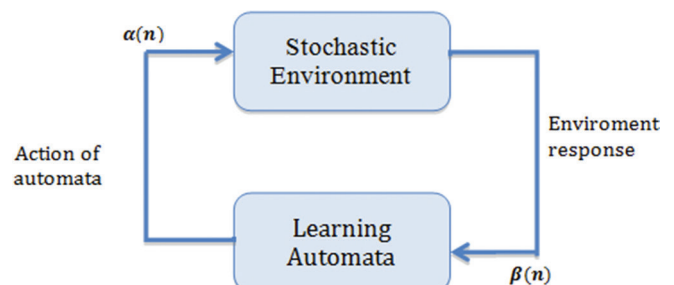


Figure 3: Learning automata and environment

current state and input to the next state. F can be defined as: $\Phi(n+1) = F(\Phi[n], \beta[n])$

- $h: \Phi \times \beta \rightarrow \alpha$ is the output function that mapping current state and input to the current output. $\alpha(n) = g(\Phi[n])$ if output function replace by $g: \Phi \rightarrow a$.

N indicates the iteration number and $P_j(n)$ is action probability; the probability that automaton is in state j at iteration n .

The automata schema can be described as follow:

If $\alpha(n) = \alpha_i$ and for $j \neq i; (j = 1 \text{ to } r)$

$$P_j(n+1) = P_j(n) - g_i(p[n]) \text{ when } \beta(n) = 0. \tag{2}$$

$$P_j(n+1) = P_j(n) - h_i(p[n]) \text{ when } \beta(n) = 1. \tag{3}$$

In order to preserve probability measure,

$$\sum_j P_j(n) = 1, \text{ or } j = 1 \text{ to } r \tag{4}$$

Region of Interest Detection Proposed Method

The proposed approach improves searching local maxima of the pixel grey level intensity (as seeds) using the method is described in section A. Then, an algorithm is represented for automatic detection of suspicious ROI. This algorithm is based on LA that is an optimization algorithm.

The proposed algorithm has been described in the following:

Begin

- 1) Threshold-based seed selection
- 2) Selecting best seeds-based on LBP feature and learning methods

Input: Original image, set of seeds
for each seed

- 3) Define a constant initial radius r_0
Calculate energy of ROI with radius r_0 (with fitness function) and
While (termination criterion not satisfied)
 %For constant number of loop (n)
- 4) Using Automata to optimize the radius of ROI detection
- 5) Calculate the fitness of ROI (energy)

End

- 5) Sorting n radius based on fitness
- 6) Selecting a best radius with high fitness
- 7) Crop the ROI with this radius from original image
- 8) Merge this ROIs with pervious ROIs

End

End

After selecting the seed point, automata need an initial radius of ROI to assign to seed. So automat starts its activity with initial radius of 1. In fact, initial ROI contains

the pixels of MRI that are in the smallest size of seed's neighborhood (3×3). The seed is the center of this ROI.

We have three actions with fair probability. At the first action, it increases the radius of ROI. The second action decreases radius and the third action doesn't change radius. LA randomly selects one of these three actions and then applied to the radius of ROI. Then, based on selected action, the radius is changed. After that, the energy of this ROI is computed. If new ROI with new radius has higher energy than previous one, the probability of selected action will be increased, otherwise will be decreased. In other word, automata use corresponding response from an environment, which is also known as reinforcement signal, to update probability of actions at each stage of order to select its next action. The procedure continues until an optimal radius for ROI obtained. So at the end of iterations the best radius is selected based on energy of pixels belong to ROI. This ROI with optimal radius is cropped from image and the next seed as a center of next ROI is selected by automata. After applying this procedure to the whole set of seeds, optimal radius of suspicious ROIs is obtained by LA for each seed. At the end, all of these ROIs are merged as suspicious ROIs.

As an example, Figure 4 reported the original image (left) and the detected ROI (right).

EXPERIMENTAL RESULTS

In the previous section, we proposed an approach for breast lesion detection in MRIs in detail. In this section, the performance of this method is investigated by using PIDER breast MRI dataset (see <https://www.imaging.ncl.nih.gov/ncia>). This dataset includes breast MRI and its ground truth (GT) segmentation that have been manually identified by a radiologist. GT is used as a reference for

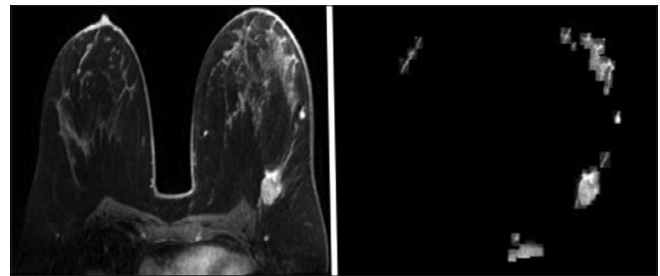


Figure 4: Original image (left), detected region of interest (right)

Table 1: Definition of some expressions

| Test outcome | Condition as determined by "radiologist" | |
|--------------|--|----------|
| | Lesion | Unlesion |
| Lesion | TP | FP |
| Unlesion | FN | TN |

TP – True positive; TN – True negative; FP – False positive; FN – False negative

performance evaluation of ROI detection methods in our experiments.

Evaluation Criteria

Several measures exist to evaluate the performance of the proposed algorithm. Among them, we chose the specificity, accuracy, and FP per image. Following, it is given a definition of some expressions in Table 1.

Accuracy

This criterion is used to measure the similarity between assigned labels by computer algorithm and real labels given by a radiologist.

$$\text{Accuracy} = \frac{TP+TN}{TP+FP+FN+TN} \tag{5}$$

Specificity

This criterion measures the proportion of negatives that are correctly identified.

$$\text{Specificity} = \frac{TN}{TN+FP} \tag{6}$$

False Positives/Image

The number of nonpathological regions detected with an algorithm as suspicious region.

Performance Evaluation of Seed Selection

After the seed selection based on thresholding, we used 100 images in size 25×25 pixel containing and not containing tumor for training the (k-NN with $k = 10$). Best seeds are selected from first set using k-NN and LBP feature (using the proposed approach). The results of these stages are shown in Table 2. As it can be seen, the average number of seeds is half compared to the stage 2. Therefore, the processing time has reduced significantly.

Parameter Definition for Learning Automata

As mentioned earlier, we want to regularize radius of ROI based on energy of pixels in the region with LA.

This algorithm gets the primary radius as input and regularizes radius of ROI by LA in some iteration. Hence, it could find desired ROI with minimizing the energy of region. In this approach, LA is learned by 100 iteration. Iteration number evaluated with three criteria: Time, true positive (TP), false negative (FN).

The best values of the iteration number for LA have been set in order to minimize the time and FN and maximize TP, synchronously. This matter is revealed in Figures 5-7. As it can be seen, the TP and FN are stable in 100th iteration. It completely obvious that in higher iteration TP increases and FN has the minimum number of pixel that are missed, but the required time significantly increases, too. So the 100th iteration is the suitable choice.

Performance Evaluation

This section describes the experimental results of proposed ROI detection algorithm on breast MRI. As mentioned earlier, ROI hunter is one of the ROI detection methods based on region growing. To compare the

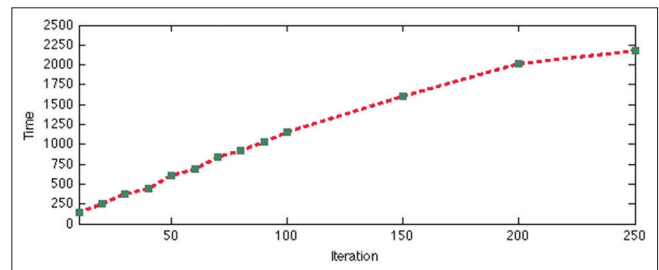


Figure 5: Required time in each iteration

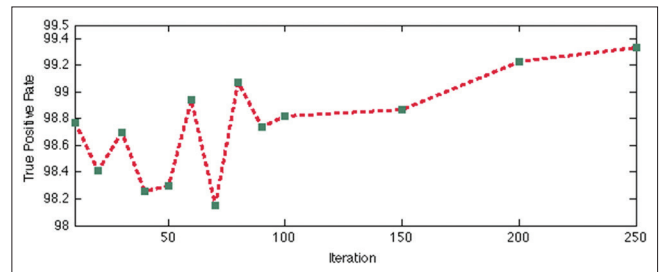


Figure 6: True positive rate of the region of interest detection in each iteration

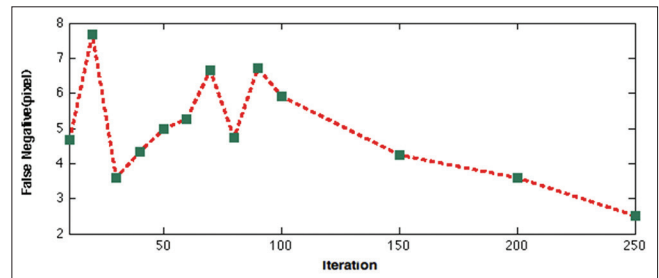


Figure 7: False negative rate of the region of interest detection in each iteration

Table 2: Seed selection results of 15 image

| Seeds | Image 1 | Image 2 | Image 3 | Image 4 | Image 5 | Image 6 | Image 7 | Image 8 | Image 9 | Image 10 | Image 11 | Image 12 | Image 13 | Image 14 | Image 15 | Mean |
|---------|---------|---------|---------|---------|---------|---------|---------|---------|---------|----------|----------|----------|----------|----------|----------|------|
| Stage 1 | 936 | 1891 | 1775 | 1100 | 1286 | 1572 | 1046 | 965 | 1634 | 1571 | 1302 | 1709 | 1076 | 996 | 1481 | 1356 |
| Stage 2 | 490 | 834 | 897 | 429 | 551 | 1033 | 715 | 313 | 1121 | 861 | 612 | 1047 | 503 | 495 | 732 | 709 |

performance of the presented method and ROI hunter, the evaluation measures such as specificity, accuracy and FP per image of these methods are computed for test data. Tables 3 and 4 represent ROI detection results of the ROI hunter and proposed approach on 15-test images. The mean, std, maximum and minimum values of

specificity, accuracy and FP for all data are also compared in Table 5.

It should be noted that the goal of this paper is to present a method to select all pathological regions without any considering of the tumor segmentation. Therefore, among

Table 3: ROI detection results of 15 image for ROI hunter

| ROI hunter | Image 1 | Image 2 | Image 3 | Image 4 | Image 5 | Image 6 | Image 7 | Image 8 | Image 9 | Image 10 | Image 11 | Image 12 | Image 13 | Image 14 | Image 15 |
|------------|---------|---------|---------|---------|---------|---------|---------|---------|---------|----------|----------|----------|----------|----------|----------|
| SPC | 50.5 | 55.22 | 52.71 | 53.19 | 54.43 | 54.42 | 55.23 | 52.04 | 52.34 | 51.64 | 53.39 | 50.8 | 55.03 | 57.94 | 55.67 |
| ACC | 67.96 | 71.28 | 69.63 | 69.91 | 70.79 | 70.8 | 71.28 | 68.78 | 69.25 | 71.15 | 73.46 | 69.61 | 67.46 | 71.5 | 70.13 |
| FP/image | 9 | 12 | 12 | 10 | 13 | 11 | 14 | 9 | 11 | 11 | 13 | 10 | 12 | 14 | 13 |

ROI – Regions of interest; SPC – Specificity; ACC – Accuracy; FP – False positive

Table 4: ROI detection results of 15 image for proposed approach

| Proposed approach | Image 1 | Image 2 | Image 3 | Image 4 | Image 5 | Image 6 | Image 7 | Image 8 | Image 9 | Image 10 | Image 11 | Image 12 | Image 13 | Image 14 | Image 15 |
|-------------------|---------|---------|---------|---------|---------|---------|---------|---------|---------|----------|----------|----------|----------|----------|----------|
| SPC | 63.61 | 59.93 | 59.47 | 60.68 | 59.7 | 58.69 | 61.47 | 55.42 | 72.06 | 61.75 | 62.12 | 60.23 | 68.40 | 57.31 | 56.32 |
| ACC | 77.72 | 74.89 | 74.64 | 75.45 | 74.75 | 73.81 | 75.8 | 70.83 | 83.33 | 77.45 | 74.32 | 72.43 | 70.79 | 81.22 | 73.16 |
| FP/image | 10 | 5 | 10 | 8 | 6 | 8 | 7 | 9 | 8 | 7 | 9 | 9 | 8 | 7 | 8 |

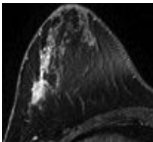
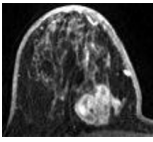
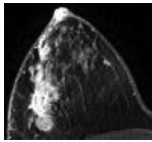
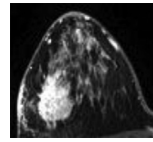
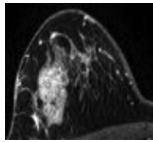
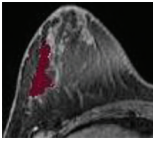
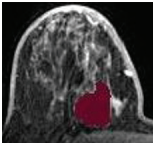
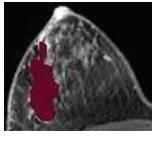
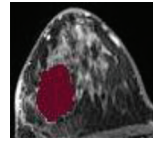
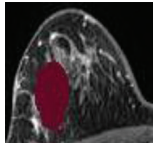
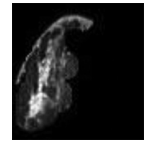
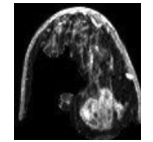
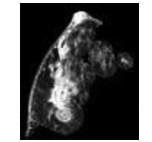
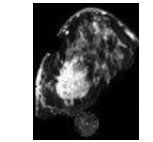
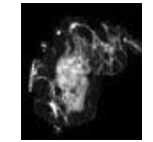
ROI – Regions of interest; SPC – Specificity; ACC – Accuracy; FP – False positive

Table 5: ROI detection results of 15 image for proposed approach and ROI hunter

| | Proposed approach | | | | ROI hunter | | | |
|----------|-------------------|--------------------|---------|---------|------------|--------------------|---------|---------|
| | Mean | Standard deviation | Maximum | Minimum | Mean | Standard deviation | Maximum | Minimum |
| SPC (%) | 61.14 | 4.35 | 72.06 | 55.42 | 53.64 | 2.03 | 57.94 | 50.5 |
| ACC (%) | 75.39 | 3.37 | 83.33 | 70.79 | 70.18 | 1.52 | 73.46 | 67.96 |
| FP/image | 7.92 | 1.44 | 10 | 5 | 11.6 | 1.64 | 14 | 9 |

ROI – Regions of interest; SPC – Specificity; ACC – Accuracy; FP – False positive

Table 6: ROI detection results for ROI hunter and proposed methods

| | ROI detection result | | | | |
|-------------------|---|---|--|---|---|
| | Test image 1 | Test image 2 | Test image 3 | Test image 4 | Test image 5 |
| Original MRI |  |  |  |  |  |
| Ground truth |  |  |  |  |  |
| Proposed approach |  |  |  |  |  |
| ROI hunter |  |  |  |  |  |

ROI – Region of interest; MRI – Magnetic resonance images

several measures, the specificity is the most important criteria, because it indicates the ability of the algorithm to select regions that contain the lesions.

Unfortunately, during the detection process, a lot of nonpathological regions are selected too. However, to get a better performance for a CAD system, the ROI is requested to admit a low number of FP. So, a proper method should maximize the specificity and minimize the FP/image number. The quantitative evaluation results of all 15-test images provided in Table 5, also the visual results for sample data illustrated in Table 6 show that the proposed method could produce more proper results compared to ROI hunter visually and in terms of specificity, accuracy and FP/image measures. It means that the regions are detected more accurately compared to the ROI hunter (The accuracy was (61.14 ± 4.35) and (53.64 ± 2.03) between computer and radiologist for proposed approach and ROI hunter respectively while FP/image was 7.92 ± 1.44 for our method and 11.6 ± 1.64 for ROI hunter).

As computation time point of view, the application of metaheuristic and soft computing techniques lead to increase the computation time in spite of high accuracy. In proposed method to extract ROI, the computation time will be increased because of using LA. To evaluate of mentioned time, 15-test images were tested by a PC of 3.2 GHZ CPU and 4 Gb RAM. The average of processing time for extract ROI is approximately 8 minutes this time is completely acceptable with respect to achieved accuracy.

CONCLUSION

In this paper, a new automatically algorithm is presented for breast lesion detection in MRIs. The algorithm is based on region growing, and it used LBP feature for accurately seed selection. It decreases the probability of selecting the noise pixel as a seed. This algorithm used learning automat and energy of image for growing the regions and was able to select regions with higher probability to contain lesions.

This method was evaluated through three criteria; accuracy, specificity, FP/image. The results show that the proposed method has the higher performance compared to ROI hunter method in detecting the suspicious region.

REFERENCES

- Warren R, Coulthard A. Breast MRI in Practice. London, UK: Martin Dunitz; 2002.
- Kerlikowske K, Carney PA, Geller B, Mandelson MT, Taplin SH, Malvin K, *et al.* Performance of screening mammography among women with and without a first-degree relative with breast cancer. *Ann Intern Med* 2000;133:855-63.
- Kolb TM, Lichy J, Newhouse JH. Comparison of the performance of screening mammography, physical examination, and breast US and evaluation of factors that influence them: An analysis of 27,825 patient evaluations. *Radiology* 2002;225:165-75.
- Bird RE, Wallace TW, Yankaskas BC. Analysis of cancers missed at screening mammography. *Radiology* 1992;184:613-7.
- Kopans DB. The positive predictive value of mammography. *AJR Am J Roentgenol* 1992;158:521-6.
- Morris EA. Diagnostic breast MR imaging: Current status and future directions. *Radiol Clin North Am* 2007;45:863-80, vii.
- Saslow D, Boetes C, Burke W, Harms S, Leach MO, Lehman CD, *et al.* American Cancer Society guidelines for breast screening with MRI as an adjunct to mammography. *CA Cancer J Clin* 2007;57:75-89.
- Berg WA, Gutierrez L, NessAiver MS, Carter WB, Bhargavan M, Lewis RS, *et al.* Diagnostic accuracy of mammography, clinical examination, US, and MR imaging in preoperative assessment of breast cancer. *Radiology* 2004;233:830-49.
- Stavros AT, Thickman D, Rapp CL, Dennis MA, Parker SH, Sisney GA. Solid breast nodules: Use of sonography to distinguish between benign and malignant lesions. *Radiology* 1995;196:123-34.
- Berriolo-Riedinger A, Touzery C, Riedinger JM, Toubeau M, Coudert B, Arnould L, *et al.* [18F] FDG-PET predicts complete pathological response of breast cancer to neoadjuvant chemotherapy. *Eur J Nucl Med Mol Imaging* 2007;34:1915-24.
- Berg WA, Weinberg IN, Narayanan D, Lobrano ME, Ross E, Amodei L, *et al.* High-resolution fluorodeoxyglucose positron emission tomography with compression ("positron emission mammography") is highly accurate in depicting primary breast cancer. *Breast J* 2006;12:309-23.
- Boetes C, Mus RD, Holland R, Barentsz JO, Strijk SP, Wobbes T, *et al.* Breast tumors: Comparative accuracy of MR imaging relative to mammography and US for demonstrating extent. *Radiology* 1995;197:743-7.
- Smith RA, Cokkinides V, Eyre HJ. Cancer screening in the United States, 2007: A review of current guidelines, practices, and prospects. *CA Cancer J Clin* 2007;57:90-104.
- Liney GP, Sreenivas M, Gibbs P, Garcia-Alvarez R, Turnbull LW. Breast lesion analysis of shape technique: Semiautomated vs. manual morphological description. *J Magn Reson Imaging* 2006;23:493-8.
- Gal Y, Mehnert A, Bradley A, McMahon K, Crozier S. Automatic segmentation of enhancing breast tissue in dynamic contrast-enhanced MR images. In: 9th Biennial Conference of the Australian Pattern Recognition Society on Digital Image Computing Techniques and Applications Glenelg, Australia; 2007. p. 124-9.
- Arbach L, Stolpen A, Reinhardt JM. Classification of breast MRI lesions using a backpropagation neural network. 2nd IEEE International Symposium on Biomedical Imaging: Macro to Nano. Piscataway, NJ, USA, Vol. 1, 2004. p. 253-6.
- Hayton P. Analysis of contrast-enhanced breast MRI. D. Phil. Department of Engineering Science, Oxford; 1998.
- Ghuijs KG, Giger ML, Bick U. A method for computerized assessment of tumour extent in contrast-enhanced MR images of the breast. Amsterdam: Elsevier; 1999. p. 305-10.
- Lucht RE, Knopp MV, Brix G. Classification of signal-time curves from dynamic MR mammography by neural networks. *Magn Reson Imaging* 2001;19:51-7.
- Yan J, Zhao B, Wang L, Zelenetz A, Schwartz LH. Marker-controlled watershed for lymphoma segmentation in sequential CT images. *Med Phys* 2006;33:2452-60.
- Cui Y, Tan Y, Zhao B, Liberman L, Parbhu R, Kaplan J, *et al.* Malignant lesion segmentation in contrast-enhanced breast MR images based on the marker-controlled watershed. *Med Phys* 2009;36:4359-69.
- Vignati A, Giannini V, De Luca M, Morra L, Persano D, Carbonaro LA, *et al.* Performance of a fully automatic lesion detection system for breast DCE-MRI. *J Magn Reson Imaging* 2011;34:1341-51.
- Renz DM, Böttcher J, Diekmann F, Poellinger A, Maurer MH, Pfeil A,

- et al.* Detection and classification of contrast-enhancing masses by a fully automatic computer-assisted diagnosis system for breast MRI. *J Magn Reson Imaging* 2012;35:1077-88.
24. Fauci F, Raso G, Magro R, Forni G, Lauria A, Bagnasco S, *et al.* A massive lesion detection algorithm in mammography. *Phys Med* 2005;21:23-30.
 25. Azmi R, Norozi N, Anbiaee R, Salehi L, Amirzadi A. IMPST: A new interactive self-training approach to segmentation suspicious lesions in breast MRI. *J Med Signals Sens* 2011;1:138-48.
 26. Ojala T, Pietikäinen M, Harwood D. A comparative study of texture measures with classification based on feature distributions. *Pattern Recognit* 1996;29:51-9.
 27. Ojala T, Pietikäinen M, Mäenpää T. Multiresolution gray-scale and rotationinvariant texture classification with local binary patterns. *IEEE Trans Pattern Anal Mach Intell* 2002;24:971-87.
 28. Heikkilä M, Pietikäinen M, Schmid C. Description of interest regions with local binary patterns. *Pattern Recognit* 2009;42:425-36.
 29. Cover M, Hart PE. Nearest neighbor pattern classification. *IEEE Trans Inf Theory* 1967;IT-13:21-7.
 30. Thathachar ML, Sastry PS. Varieties of learning automata: An overview. *IEEE Trans Syst Man Cybern B Cybern* 2002;32:711-22.

How to cite this article: Salehi L, Azmi R. A Novel Method Based on Learning Automata for Automatic Lesion Detection in Breast Magnetic Resonance Imaging. *J Med Sign Sence* 2014;4:202-10.

Source of Support: Nil, **Conflict of Interest:** None declared

BIOGRAPHIES



Leila Salehi received the B.Sc degree in computer engineering from Abhar University, Zanjan, Iran in 2007. Currently she is doing MASC in Artificial Intelligence from Alzahra University, Tehran, Iran. Her research interests include Medical Image processing, Machine Vision.

E-mail: salehi.leili@gmail.com



Reza Azmi received his BS degree in Electrical Engineering from Amirkabir university of technology, Tehran, Iran in 1990 and his MS and PhD degrees in Electrical Engineering from Tarbiat Modares university, Tehran, Iran in 1993

and 1999 respectively. Since 2001, he has joined Alzahra university, Tehran, Iran. He was an expert member of Image Processing and Multi-Media working groups in ITRC (From 2003 to 2004), Optical Character Recognition working group in supreme council of information and communication technology (From 2006 to 2007) and Security Information Technology and Systems working groups in ITR (From 2006 to 2008). He was Project Manager and technical member of many industrial projects.

E-mail: azmi@alzahra.ac.ir